

# The dispersion of a single hole in an antiferromagnet

Andrey V. Chubukov and Dirk K. Morr

Department of Physics, University of Wisconsin-Madison, 1150 University Ave., Madison, WI 53706  
(March 12, 2018)

We revisit the problem of the dispersion of a single hole injected into a quantum antiferromagnet. We applied a spin-density-wave formalism extended to large number of orbitals and obtained an integral equation for the full quasiparticle Green's function in the self-consistent “non-crossing” Born approximation. We found that for  $t/J \gg 1$ , the bare fermionic dispersion is completely overshadowed by the self-energy corrections. In this case, the quasiparticle Green's function contains a broad incoherent continuum which extends over a frequency range of  $\sim 6t$ . In addition, there exists a narrow region of width  $O(JS)$  below the top of the valence band, where the excitations are mostly coherent, though with a small quasiparticle residue  $Z \sim J/t$ . The top of the valence band is located at  $(\pi/2, \pi/2)$ . We found that the form of the fermionic dispersion, and, in particular, the ratio of the effective masses near  $(\pi/2, \pi/2)$  strongly depend on the assumptions one makes for the form of the magnon propagator. We argue in this paper that two-magnon Raman scattering as well as neutron scattering experiments strongly suggest that the zone boundary magnons are not free particles since a substantial portion of their spectral weight is transferred into an incoherent background. We modeled this effect by introducing a cutoff  $q_c$  in the integration over magnon momenta. We found analytically that for small  $q_c$ , the strong coupling solution for the Green's function is universal, and both effective masses are equal to  $(4JS)^{-1}$ . We further computed the full fermionic dispersion for  $J/t = 0.4$  relevant for  $Sr_2CuO_2Cl_2$ , and  $t' = -0.4J$  and found not only that the masses are both equal to  $(2J)^{-1}$ , but also that the energies at  $(0, 0)$  and  $(0, \pi)$  are equal, the energy at  $(0, \pi/2)$  is about half of that at  $(0, 0)$ , and the bandwidth for the coherent excitations is around  $3J$ . All of these results are in full agreement with the experimental data. Finally, we found that weakly damped excitations only exist in a narrow range around  $(\pi/2, \pi/2)$ . Away from the vicinity of  $(\pi/2, \pi/2)$ , the excitations are overdamped, and the spectral function possesses a broad maximum rather than a sharp quasiparticle peak. This last feature was also reported in photoemission experiments.

## I. INTRODUCTION

The dispersion of a single hole in a quantum antiferromagnet is one of the issues in the field of high-temperature superconductivity which has attracted a substantial amount of interest over a number of years [1–19]. The parent compounds of the high- $T_c$  materials are quantum Heisenberg antiferromagnets as was demonstrated by neutron scattering [21], NMR [22] and Raman [23] experiments. The antiferromagnetic spin ordering strongly modifies the electronic dispersion which by all accounts is very different from what one would expect from band theory calculations. Upon hole doping, short-range antiferromagnetism gradually disappears, and the overdoped cuprates possess an electronic dispersion which is consistent with band theory predictions [25]. How the electronic spectrum evolves with doping is currently a subject of intensive experimental and theoretical studies [26–29]. As an important input for these studies, one needs to know what happens in the limit of zero doping when a single hole is injected into a quantum antiferromagnet.

The dispersion of a single hole in an antiferromagnet has been intensively studied experimentally and theoretically. Experimental information comes from photoemission experiments on the half-filled  $Sr_2CuO_2Cl_2$  which is not a high- $T_c$  superconductor, but contains the same

$CuO_2$  planes as the high- $T_c$  materials [30,31]. Most of the theoretical analysis was performed in the framework of the  $t - J$  and Hubbard models which are widely believed to adequately describe the low-energy physics of the underlying three-band model [1–13,15–19]. Early analytical and numerical computations were performed in the antiferromagnetically ordered phase and for the case when a hopping is only possible between nearest neighbors [1–3,5,12,13]. These studies have shown that in the strong coupling limit (large  $U$  limit in the Hubbard model or  $t \gg J$  limit in the  $t - J$  model), the Green's function of a single hole has the form

$$G(k, \omega) = \frac{Z}{\omega - E_k} + G_{inc}(k, \omega), \quad (1)$$

where the coherent part is confined to scales smaller than  $2J$ , while the incoherent background stretches up to a few  $t$ . The quasi-particle residue of the coherent piece is small and scales as  $Z \propto J/t$  in the limit  $t \gg J$ . The dispersion  $E_k$  has a maximum at  $k = (\pi/2, \pi/2)$  and symmetry related points. All calculations have demonstrated that the dispersion around this point is very anisotropic with a substantially larger mass along the  $(0, \pi)$  to  $(\pi, 0)$  direction than along the Brillouin zone diagonal. For  $t/J = 2.5$  relevant to cuprates, the ratio of the masses is about 5 – 7 in the  $t - J$  model (without a three-site term) [3], and it is even larger in the Hubbard model due to the presence of the bare dispersion  $J(\cos k_x + \cos k_y)^2$

which yields an extra contribution to the mass along the zone diagonal [20].

It turns out, however, that the experimental results for  $Sr_2CuO_2Cl_2$  [31,30] are rather different from these predictions. Although the photoemission data have demonstrated that the maximum of  $E_k$  is at  $k = (\pi/2, \pi/2)$  consistent with the theory, the experimentally measured ratio of the masses is close to one in clear disagreement with the theoretical predictions. Moreover, the data show that the coherent peak in the spectral function exists only in a narrow region around  $(\pi/2, \pi/2)$  while away from this region, the hole spectral function is nearly featureless. This implies that the fermionic excitations become overdamped already at energies which are substantially smaller than  $2J$ .

After the data were reported, several attempts have been made to improve the agreement between theory and experiment. One scenario was put forward by researchers working on the “gauge theory” approach to cuprates [32], most recently by Laughlin [33]. He argued that the isotropy of the dispersion together with the observed mostly incoherent nature of the electronic excitations are signatures of a spin-charge separation. For a state where spin and charge degrees of freedom are described by separate quasiparticles (spinons and holons, respectively), the electron Green’s function is just a convolution of the spinon and holon propagators. It does not have a pole which normally would be associated with the coherent part of  $G(k, \omega)$ , but rather a branch cut which describes fully incoherent excitations. Laughlin argued that since spinon and holon energies are well separated (the spinon energy has an overall scale of  $J$ , while the holon energy is  $O(t)$ ), the position of the branch cut virtually coincides with the spinon dispersion. In the mean-field theory for the spin-charge separated state, the spinon energy has the form

$$E_k^{spinon} = -C_{sw}(\cos^2 k_x + \cos^2 k_y)^{1/2}, \quad (2)$$

where  $C_{sw} \sim 1.6J$  is the spin-wave velocity in a 2D  $S = 1/2$  antiferromagnet. This dispersion has an isotropic maximum at  $k = (\pi/2, \pi/2)$ , a bandwidth of  $2.2J$  and equal energies for  $k = (0, 0)$  and  $(0, \pi)$  - all of these features are consistent with the data together with the near absence of the quasiparticle peak.

An obvious weakness of the mean-field analysis of spinons and holons is that it neglects the effects due to a gauge field. Beyond the mean-field level, a gauge field may glue spinons and holons into a bound state thus rendering the electron as a coherent quasiparticle. Laughlin conjectured that the confinement takes place only below  $T_N$ , while the experimental data were actually collected at  $T = 350K$  which is  $100K$  above the Neel temperature. He then proposed that if measurements are done at much lower temperatures, they should yield an anisotropic dispersion consistent with the results obtained in the ordered state with no spin-charge separation.

Another, more conventional approach to the single hole problem assumes that there is no spin-charge separation

at any  $T$ , and that the experimental data in fact reflect the behavior of the hole dispersion in the antiferromagnetically ordered phase [15–19]. Within this approach, the discrepancy with the data is mainly attributed to the fact that the original model did not contain a hopping term  $t'$  between next-nearest neighbors (and, possibly, also between further neighbors). The presence of the a finite  $t'$  term in the Hubbard model is justified, at least partly, by studies which derived an effective one-band model from the underlying three-band model by comparing the energy levels around the charge transfer gap [34]. These studies predicted that the second-neighbor hopping is about  $t' = -0.2t$ . By itself, this hopping is small compared to  $t$ . However, in an antiferromagnetic background, the hole can only move within the same sublattice, otherwise the antiferromagnetic ordering is disturbed. The hopping term  $t'$  connects the sites within the same sublattice, and therefore is not affected by antiferromagnetism. On the contrary, the  $t$  term contributes to the hopping within a sublattice only via the creation of a virtual doubly occupied state which costs the energy  $U$ . As a result, the  $t$ -part of the dispersion is rescaled and becomes of order  $t^2/U = O(J)$ . One therefore has to compare  $t'$  not with  $t$  but rather with  $J$ . For  $J/t \sim 0.4$ , we then obtain  $t' = -0.5J$ , which immediately implies that the corrections due to  $t'$  are actually quite relevant.

It has been mentioned several times in the literature that the inclusion of  $t' = -0.5J$  into the Hubbard model yields a good agreement with the experimental data already at the mean-field level [15,16]. Indeed, the mean-field spin-density-wave (SDW) formula for the hole dispersion at large  $U$  is

$$E_k = -J(\cos k_x + \cos k_y)^2 - 4t' \cos k_x \cos k_y. \quad (3)$$

For  $t' = -0.5J$ , this formula transforms into

$$E_k = -J(\cos^2 k_x + \cos^2 k_y) \quad (4)$$

(here we assumed that the chemical potential is at the top of the valence band). This dispersion possesses two equal effective masses if one expands around the maximum at  $(\pi/2, \pi/2)$ , and has a local maximum at  $(0, \pi/2)$  with  $E = -J$ . Both of these results are consistent with the most recent data by LaRosa *et al.* [31]. Furthermore, the data show that the energies at  $(0, 0)$  and  $(0, \pi)$  are both equal to  $-2J$ . This also agrees with the photoemission data [30,31].

The conventional mean-field SDW-type approach also possesses the weakness that it predicts fully coherent excitations upto  $2J$ . The data, however, demonstrate that away from the vicinity of  $(\pi/2, \pi/2)$ , the coherent part of the dispersion is almost completely overshadowed by the incoherent background. Earlier studies [15] which went beyond the mean-field level have demonstrated that self-energy corrections reduce the quasiparticle residue thus transferring part of the spectral weight into the incoherent background. However, these corrections also effectively decrease  $t'$  and thus render the spectrum more

anisotropic (see Fig. 11 and 13 below). From this perspective, the observed isotropy of the dispersion around  $(\pi/2, \pi/2)$  is attributed in a conventional approach to some fine tuning of both  $J/t$  and  $t'/J$  and is therefore completely accidental [35].

In this paper we show that in a certain limit specified below, the near-degeneracy of the spectrum around  $(\pi/2, \pi/2)$  turns out to be a fundamental, universal property of a single hole in an antiferromagnet, independent of the details of the physics at atomic scales. Our key point is this: in all previous studies which yielded anisotropic spectra, it was assumed that magnons behave as free particles for all momenta. In this case, the integral over the magnon momenta in the self-energy term runs over the whole magnetic Brillouin zone (MBZ). On the other hand, Raman studies of the two-magnon profile in the insulating parent compounds of high  $T_c$  materials have demonstrated that the width of the two-magnon peak is much broader than one would expect for free magnons [23,24]. The dominant contribution to this peak comes from the magnons near the boundary of the MBZ. Complimenting these findings, neutron scattering experiments on  $La_2CuO_4$  [36] have shown that about half of the spectral weight of the quasiparticle peak for the zone boundary magnons is transferred into a broad incoherent background.

It has been suggested that the broadening is due to the strong interaction between these magnons and phonons [37,38]. This interaction is finite and not necessary small at  $T = 0$  contrary to the magnon-magnon interaction which gives rise to an incoherent part of the magnon spectral function only at finite  $T$  and is irrelevant for  $T \ll J$  [39].

In this situation, it seems reasonable to assume that the contribution from the zone boundary magnons to the electronic self-energy is substantially reduced compared to what one would obtain for free spin waves. This however is true only for zone-boundary magnons. For long-wavelength magnons, the magnon-phonon vertex scales linearly with the magnon momentum, and the incoherent part of the magnon propagator is small. The simplest way to model this effect is to introduce an upper cutoff  $q_c$  in the integration over magnon momenta. Naively, one might expect that the hole dispersion would strongly depend on  $q_c$ . However, we will demonstrate that at large  $t/J$ , when the bare dispersion is irrelevant, only the quasiparticle residue does depend on  $q_c$ , while the effective masses are in fact independent of  $q_c$  in the limit when  $q_c$  is sufficiently small. We explicitly show that in this limit, both masses turn out to be equal to  $1/2J$ . The dispersion near  $(\pi/2, \pi/2)$  is then isotropic and has a form  $E_k = -J\tilde{k}^2$  where  $\tilde{k}$  is the deviation from  $(\pi/2, \pi/2)$ . Furthermore, we show that for a certain range of  $q_c$  the inclusion of  $t' = -0.5J$  extends the region where the two masses are approximately equal to basically all values of  $t/J$ . This last result allows us to correctly reproduce the measured hole dispersion in  $Sr_2CuO_2Cl_2$ .

The paper is organized as follows. In the next section, we outline the formalism and derive the integral equation for the quasiparticle Green's function by expanding around the mean-field SDW solution. In Sec. III we present our analytical results in the large  $t/J$  limit. In this section we also discuss the role of the vertex corrections to the spin-fermion vertex. In Sec. IV, we present the results of the numerical solution of the self-consistency equation for the quasiparticle Green's function for different values of  $J/t$ . Sec. V contains a summary of our results.

## II. THE FORMALISM

As mentioned in the introduction, our starting point for the description of the insulating parent compounds of the high- $T_c$  materials is the effective 2D one-band Hubbard model [40–42], given by

$$\mathcal{H} = - \sum_{i,j} t_{i,j} c_{i,\alpha}^\dagger c_{j,\alpha} + U \sum_i c_{i,\uparrow}^\dagger c_{i,\uparrow} c_{i,\downarrow}^\dagger c_{i,\downarrow}. \quad (5)$$

Here  $\alpha$  is the spin index and  $t_{i,j}$  is the hopping integral which we assume to act between nearest and next-nearest neighbors ( $t$  and  $t'$ , respectively). Throughout the paper we assume that the ground state of the Hubbard model is antiferromagnetically ordered. In this situation, a way to calculate the spectral function in a systematic perturbative expansion is to extend the Hubbard model to a large number of orbitals,  $n = 2S$ , and use a  $1/S$  expansion around the mean-field SDW state [43]. The  $1/S$  expansion for the Hubbard model has been discussed several times in the literature [15,28] and we will use it here without further clarification. To obtain the mean-field solution, one introduces an antiferromagnetic long range order parameter  $S_z = \langle c_k^\dagger c_{k+Q} \rangle$  and uses it to decouple the interaction term in Eq.(5). Diagonalizing then the quadratic form by means of a unitary transformation one obtains two electronic bands for the conduction and valence fermions, whose energy dispersion is given by

$$E_k^{c,v} = \pm \sqrt{(\epsilon_k^-)^2 + \Delta^2} + \epsilon_k^+, \quad (6)$$

where

$$\epsilon_k^\pm = \frac{\epsilon_k \pm \epsilon_{k+Q}}{2} \quad \Delta = U \langle S_z \rangle$$

$$\epsilon_k = -4\bar{t}S(\cos k_x + \cos k_y) - 8\bar{t}'S \cos k_x \cos k_y - \mu. \quad (7)$$

Here  $E_k^{c,v}$  is the dispersion of the conduction and valence fermions, respectively,  $\epsilon_k$  is the dispersion of free fermions,  $\mu$  is the chemical potential, and  $\langle S_z \rangle$  is the sublattice magnetization. To facilitate the  $1/S$  expansion, we also introduced  $\bar{t} = t/2S$  and  $\bar{t}' = t'/2S$ . In the large- $U$  limit which we only consider, one can expand the square root and obtains

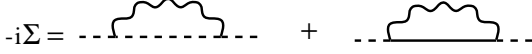


FIG. 1. The lowest order self-energy correction for the valence fermions in the SDW model. The solid and dashed lines are the bare propagators of conduction and valence fermions, respectively. The wavy line describes transverse spin fluctuations.

$$E_k^{c,v} = \pm \Delta \pm 2JS(\cos k_x + \cos k_y)^2 - 8\bar{t}'S \cos k_x \cos k_y - \mu, \quad (8)$$

where  $J = 4\bar{t}^2/U$ . At half-filling, the chemical potential can be set to the top of the valence band ( $\mu = -\Delta$ ); for  $S = 1/2$  we then reproduce Eq.(3) from the introduction.

At infinite  $S$ , the mean-field approach is exact. At finite  $S$ , the bare Green's function is renormalized due to the interaction with spin waves. The lowest order self-energy corrections for valence fermions are given by the diagrams in Fig. 1. The solid and dashed lines in these diagrams are the propagators of conduction and valence fermions, respectively. The wavy lines describe transverse spin fluctuations which in the SDW approach are collective modes of electrons. These collective modes correspond to the poles of the transverse susceptibility, and are obtained by summing up an infinite RPA series in the particle-hole channel with the total momentum equal to either zero or  $Q$ . The interaction vertices between fermionic quasiparticle and magnons have been calculated previously [44]. In the strong coupling limit they are given by

$$\begin{aligned} \Phi_{cc,vv}(k, q) &= \left[ \pm \left( \epsilon_k^{(-)} + \epsilon_{k+q}^{(-)} \right) \eta_q + \left( \epsilon_k^{(-)} - \epsilon_{k+q}^{(-)} \right) \bar{\eta}_q \right], \\ \Phi_{cv,vc}(k, q) &= U \left[ \eta_q \mp \bar{\eta}_q \right]. \end{aligned} \quad (9)$$

where  $\eta_q$  and  $\bar{\eta}_q$  are given by

$$\eta_q = \sqrt{S} \left( \frac{1 + \nu_q}{1 - \nu_q} \right)^{1/4}; \quad \bar{\eta}_q = \sqrt{S} \left( \frac{1 - \nu_q}{1 + \nu_q} \right)^{1/4}, \quad (10)$$

and  $\nu_q = (\cos q_x + \cos q_y)/2$ .

We see that there are two types of vertices:  $\Phi_{cv,vc}$  which describes the interaction between conduction and valence fermions, and  $\Phi_{cc,vv}$  which involves either only valence or only conduction fermions. Apparently, the second diagram in Fig. 1 is more relevant since the vertex which involves both conduction and valence fermions scales as  $U$ . However, incident and intermediate fermions in this diagram belong to different bands and are therefore separated by a large, momentum independent gap  $\Delta \sim US$ . As a result, the first diagram mostly contributes to the gap renormalization, which is exactly cancelled by a renormalization of  $\langle S_z \rangle$  such that the fully renormalized gap equals  $2US$  as it indeed should be for the large  $U$  Hubbard model [15,44]. Expanding this diagram in  $J/U$ , we also obtain a momentum dependent

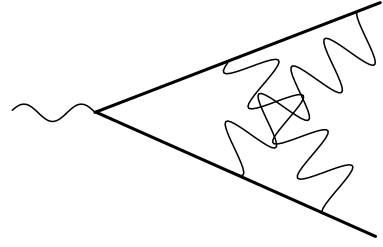


FIG. 2. The lowest order vertex correction for the vertex between fermions and transverse spin fluctuations. The diagram with only one wavy line is absent in the ordered state as it does not conserve the spin.

term of  $O(J)$  which contributes a regular  $1/S$  correction to the bare dispersion.

The first diagram in Fig. 1 involves only valence fermions. Here the vertex is reduced from  $U$  due to the coherence factors and scales as  $t$ . At the same time, both incident and internal quasiparticles are only  $O(J)$  away from the Fermi surface which implies that the denominator scales as  $J$ . The total contribution from the second diagram then behaves as  $JS(t/J\sqrt{S})^2$  and in addition is strongly momentum dependent. Since the bare dispersion is of order  $JS$ , the relative self-energy correction from the second diagram scales as  $(t/J\sqrt{S})^2$  and is small only for extremely large  $S$ . For physically relevant values of the spin, the expansion parameter is obviously large, and one certainly cannot restrict with the second order in perturbation theory.

We now formulate precisely under which conditions we carry out the calculations. We assume that  $S \gg 1$  and neglect all regular corrections in  $1/S$ . At the same time, we assume that  $t/J\sqrt{S} \gg 1$  and sum up an infinite series of diagrams in this parameter. The restriction to large  $S$  allows us not only to neglect the self-energy diagrams which involve both valence and conduction fermions, but also to neglect the quantum corrections to the spin-wave propagator. At half-filling, these regular  $1/S$  corrections can, with good accuracy, be absorbed into the renormalization of the hopping term and the exchange interaction which are both input parameters for our calculations.

The next step is to select the series of diagrams which have to be summed up. To lowest order in perturbation theory, both self-energy and vertex corrections are equally relevant: the self-energy correction yields a relative contribution of  $(\bar{t}/J\sqrt{S})^2$ , while the leading order vertex correction shown in Fig. 2 yields a relative factor  $(\bar{t}/J\sqrt{S})^4$  which is even larger. This result, however, changes if we estimate the strength of the self-energy and vertex corrections in a self-consistent manner, i.e., by considering all internal Green's functions and all vertices in the diagrams in Figs. 1 and 2 as full ones. This in turn yields self-consistent equations for the full self-energy and the full vertex. Our self-consistent calculation of the self-energy correction is similar to the one performed by Kane, Lee and Read (KLR) [2]. Follow-

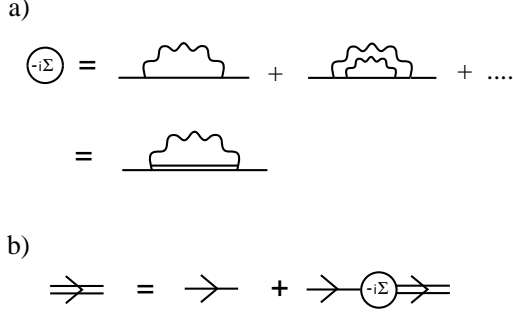


FIG. 3. a) The self-energy is given by an infinite sum of “non-crossing” diagrams. b) The Dyson equation which together with the self-energy in a) yields Eq.(11).

ing KLR, we assume that the dominant pole approximation for the full fermionic Green’s function is valid upto energies of the order of the typical spin wave energy, i.e., the full Green’s function can be approximated as  $Z/(\omega - E_k)$  where  $E_k = O(JS)$  (we later confirm this result by explicit calculations). Substituting this form into the self-energy term and performing standard manipulations we obtain for  $\bar{t}/J\sqrt{S} \gg 1$  the self-consistency condition  $\bar{t}^2 Z^2 \Phi / J^2 S \sim 1$ , where  $\Phi$  stands for the vertex renormalization. It is essential that there is only one power of  $\Phi$  in this relation as only one of the two vertices in the self-energy diagram gets renormalized. On the other hand, in the vertex correction diagram, all vertices should be considered as full ones, and the self-consistency condition yields  $(\bar{t}^2 Z^2 \Phi / J^2 S)^2 \Phi^2 \sim 1$ . Comparing these two conditions, we obtain  $Z \sim J\sqrt{S}/t$  and  $\Phi = O(1)$ . The result for  $Z$  is consistent with the one obtained by KLR. Clearly then, the self-energy corrections are more relevant than the vertex corrections since the former reduce the quasiparticle residue to a parametrically small value, while the latter only change the vertex by a factor of order  $O(1)$ . Though the vertex corrections do not contain a factor  $1/S$ , it seems reasonable to assume that they just change the overall amplitude of the vertex but do not introduce any new physics. We therefore first neglect all vertex corrections and obtain the full self-energy and thus the full Green’s function in the self-consistent Born approximation [45]. We then use the solution for the full Green’s function to estimate the relative strength of the vertex corrections. We find that the vertex corrections change the vertex by roughly 20% and therefore can be neglected with reasonable accuracy.

In the Born approximation, the full self-energy is diagrammatically given by an infinite series of “non-crossing” diagrams (see Fig. 3a). Summing up this series, we obtain that the full self-energy has the same form as in second-order perturbation theory, but the Green’s function for the intermediate fermion is now replaced by the full one. The full Green’s function is then obtained from the Dyson equation (see Fig. 3b) and is analytically given by

$$G^{-1}(k, \omega) = \omega - (E_k^v - \mu) - \int \frac{d^2 q}{4\pi^2} d\Omega \Psi(k, q) G(k + q, \omega + \Omega) F(q, \Omega), \quad (11)$$

where  $F(q, \omega)$  is the spin-wave propagator, and

$$\begin{aligned} \Psi(k, q) &= \Phi_{vv}^2 = 32S\bar{t}^2 \left[ \nu_k^2 + \nu_{k+q}^2 - 2\nu_k \nu_q \nu_{k+q} \right. \\ &\quad \left. + \sqrt{1 - \nu_q^2} (\nu_{k+q}^2 - \nu_k^2) \right] / \sqrt{1 - \nu_q^2}. \end{aligned}$$

The integration over the magnon momentum runs over the whole MBZ.

Eq.(11) is similar to the one derived earlier for the  $t - J$  model [2,3,45] with the only difference that Eq.11 contains the bare dispersion  $E_k^v$ . This dispersion is indeed also present when one derives the  $t - J$  model from the Hubbard model at large  $U$ . However, it is due to the three-site term which is usually omitted in the effective  $t - J$  Hamiltonian [46].

As we discussed in the introduction, the quasiparticle spectral weight of the short-wavelength magnons in the parent compounds of the high- $T_c$  materials is likely to be strongly reduced as demonstrated by Raman and neutron scattering experiments. To account for this effect, we adopt a semi-phenomenological approach and introduce a cutoff,  $q_c$ , in the integration over magnon momenta in the r.h.s. of Eq.(11). We assume that for  $q > q_c$ , the magnon spectral weight disappears into a broad background, and neglect the contribution to the self-energy from these  $q$ . On the other hand, for  $q < q_c$ , we assume that the magnons are just free particles. Furthermore, for our analytical considerations, we will assume that  $q_c$  is rather small such that we can expand the dispersion of fermions and the spin-fermion vertex to linear order in the magnon momentum. This last assumption is not well justified as the magnitude of  $q_c$  is unknown. Notice, however, that expanding upto leading order in  $q_c$ , we obtain two equal effective masses which are universal and independent of  $q_c$ . The smallness of  $q_c$  is then only needed for the corrections to these universal results to be small.

For free spin waves, we have

$$F(q, \Omega) = \frac{1}{\Omega - \omega_q + i\delta}, \quad (12)$$

where  $\omega_q = 4JS\sqrt{1 - \nu_q^2}$  is the spin-wave spectrum. The magnon propagator has a pole in the lower half-plane of  $\Omega$ . In this half-plane, the mean-field fermionic Green’s function  $G(k, \omega) = (\omega - (E_k^v - \mu) + i\delta \text{sgn}\omega)^{-1}$  is free from nonanalyticities since  $E_k^v - \mu < 0$ . We assume, following KLR, that the full  $G(k, \omega)$  is also analytic in the lower half-plane of  $\Omega$ . Then one can straightforwardly perform the integration over magnon frequency in Eq.(11) and obtain

$$\begin{aligned} G^{-1}(k, \omega) &= \omega - (E_k^v - \mu) \\ &\quad - \int \frac{d^2 q}{4\pi^2} \Psi(k, q) G(k + q, \omega + \omega_q). \end{aligned} \quad (13)$$

We first present our analytical results for the full Green's function in certain limiting cases, and then present the full numerical solution of Eq.(13).

### III. ANALYTICAL RESULTS

We obtain the analytical solution of Eq.(13) in two different ranges of  $\omega$ . In Sec. III A we first solve the self-consistency equation in the limit  $|\omega - \omega_{max}| \gg \Lambda$ , where  $\omega_{max}$  is the highest frequency at which the full Green's function first acquires a finite imaginary part, and  $\Lambda = JS(\bar{t}/J\sqrt{S})^{1/3}$ . We show that for  $|\omega - \omega_{max}| \gg \Lambda$  the excitations are purely incoherent and extend over a region of  $\sim 6\bar{t}\sqrt{2S}$ . In Sec. III B we then consider the case  $|\omega - \omega_{max}| \leq \Lambda$ . In this frequency range we find coherent excitations which exist up to energies of  $O(JS)$  down from the maximal frequency.

#### A. Incoherent part of the excitation spectrum

We first observe that the interaction vertex in Eq.(13) has an overall scale of  $(\bar{t}\sqrt{S})^2$ , while the quasiparticle Green's function behaves as  $1/\omega$  at very large frequencies (here, and in the following, we shifted the frequency by the mean-field chemical potential,  $\mu = -\Delta$ ). Obviously than, for  $\omega \gg t\sqrt{S}$ , the perturbative expansion in the spin-fermion interaction is convergent, and the density of states (DOS) is exactly equal to zero, as in the mean-field theory. When  $\omega$  is reduced to the scale of  $\bar{t}\sqrt{S}$ , the lowest-order self-energy term  $\sim \bar{t}^2 S/\omega$  becomes of the same magnitude as the frequency in the bare Green's function, i.e., the expansion parameter is  $O(1)$ . We show that in this frequency range there exists a critical value of  $\omega$  below which perturbation theory becomes non-convergent and there appears a finite DOS. It is essential that for small  $J\sqrt{S}/\bar{t}$ , the critical frequency is still much larger than the magnon frequency such that one can neglect  $\omega_q$  and  $E_k^v$  compared to  $\omega$  in the r.h.s. of Eq.(13). The self-consistency equation then reduces to a conventional integral equation

$$G^{-1}(k, \omega) = \omega - \int \frac{d^2 q}{4\pi^2} \Psi(k, q - k) G(q, \omega) \quad (14)$$

in which the dependence on the external momentum is only present in the interaction vertex. Furthermore, we assume that  $\omega \sim \bar{t}\sqrt{S}$  is larger than the total magnon bandwidth, including the incoherent part. In this situation, the integration over  $q$  runs over the whole MBZ.

Before we present the solution of Eq.(14), it is instructive to consider a simplified version of this equation in which  $\Psi(k, q - k)$ , which is a smooth function of the fermionic momentum, is just substituted by some constant  $\sim \bar{t}^2 S$ . The equation for the full  $G(\omega)$  then reduces to

$$G^{-1}(\omega) = \omega - \bar{t}^2 S G(\omega), \quad (15)$$

where  $\bar{t}/\bar{t} = O(1)$ . Solving this algebraic equation, we obtain for positive  $\omega$

$$G(\omega) = \frac{2}{\omega + \sqrt{\omega^2 - \omega_{max}^2}}, \quad (16)$$

where  $\omega_{max} = 2\bar{t}\sqrt{S}$ . We see that for  $\omega > \omega_{max}$ , the Green's function is real. This is the frequency range where perturbation theory is valid. For  $\omega < \omega_{max}$ , however, the expression under the square root is negative, and the solution possesses a finite imaginary part which gives rise to a finite DOS. The total width of the DOS is obviously  $W = 2\omega_{max} = 4\bar{t}\sqrt{S}$ .

We now solve Eq.(14) with the actual  $\Psi(k, q - k)$ . We introduce a new function  $f_k(\omega)$  via

$$G_k^{-1}(\omega) = \omega f_k(\omega^2). \quad (17)$$

Substituting this into Eq.(14), we obtain

$$f_k = 1 - \alpha \int \frac{d^2 q}{4\pi^2 f_q} \left[ \nu_q^2 - \nu_k^2 + \frac{\nu_k^2 + \nu_q^2 - 2\nu_k \nu_q \nu_{q-k}}{\sqrt{1 - \nu_{q-k}^2}} \right], \quad (18)$$

where we defined  $\alpha = 32\bar{t}^2 S/\omega^2$ .

The general solution of Eq.(14) can be obtained by expanding in the eigenfunctions of the  $D_{4h}$  symmetry group of the square lattice. The solution is in general rather cumbersome because the vertex contains a  $k$ -dependent term in the denominator. However, it is easy to verify that the expression in the square brackets vanishes when  $\nu_{q-k} \rightarrow 1$ . The dominant contribution to the r.h.s. of Eq.(14) then comes from the region of  $q$ -space where  $\nu_{q-k}$  is relatively small i.e., the denominator is close to one. For simplicity, we just set it equal to one. We then obtain

$$f_k = 1 - \alpha \int \frac{d^2 q}{4\pi^2 f_q} \nu_q [\nu_q - \nu_k \nu_{q-k}]. \quad (19)$$

This equation is much simpler to solve because the decomposition of  $\nu_{q-k}$  into the eigenfunctions of the square lattice involves only four eigenfunctions:

$$\nu_{k-q} = \nu_k \nu_q + \tilde{\nu}_k \tilde{\nu}_q + \bar{\nu}_k \bar{\nu}_q + \bar{\bar{\nu}}_k \bar{\bar{\nu}}_q, \quad (20)$$

where

$$\begin{aligned} \nu_k &= \frac{1}{2}(\cos k_x + \cos k_y); & \tilde{\nu}_k &= \frac{1}{2}(\cos k_x - \cos k_y); \\ \bar{\nu}_k &= \frac{1}{2}(\sin k_x + \sin k_y); & \bar{\bar{\nu}}_k &= \frac{1}{2}(\sin k_x - \sin k_y). \end{aligned} \quad (21)$$

We now choose a general ansatz for  $f_k$  consistent with Eq.(19)

$$f_k = A + B \nu_k^2 + C \nu_k \tilde{\nu}_k + D \nu_k \bar{\nu}_k + E \nu_k \bar{\bar{\nu}}_k \quad (22)$$

and solve this set of self-consistent algebraic equations for the coefficients. We found that the coefficients  $C, D$  and  $E$  are equal to zero, while  $A$  and  $B$  are the solutions of two coupled equations

$$\begin{aligned} A &= 1 - 2\alpha \int \frac{d^2q}{4\pi^2} \frac{\nu_q^2}{A + B\nu_q^2}, \\ B &= 2\alpha \int \frac{d^2q}{4\pi^2} \frac{\nu_q^2}{A + B\nu_q^2}. \end{aligned} \quad (23)$$

Introducing  $A = 1 - 2\alpha x, B = 2\alpha x$  and separating real and imaginary parts of  $x$  by introducing  $x = x_1 + ix_2$ , we obtain an equivalent set of equations for  $x_1$  and  $x_2$

$$\begin{aligned} x_1 &= \int \frac{d^2q}{4\pi^2} \frac{\nu_q^2 (1 - 2\alpha x_1(1 - \nu_q^2))}{[1 - 2\alpha x_1(1 - \nu_q^2)]^2 + 4\alpha^2 x_2^2(1 - \nu_q^2)^2}, \\ x_2 &= \int \frac{d^2q}{4\pi^2} \frac{\nu_q^2 (1 - \nu_q^2)(2\alpha x_2)}{[1 - 2\alpha x_1(1 - \nu_q^2)]^2 + 4\alpha^2 x_2^2(1 - \nu_q^2)^2}. \end{aligned} \quad (24)$$

In terms of  $x_1$  and  $x_2$ , the quasiparticle Green's function is given by

$$G(k, \omega) = \frac{1}{\omega} \frac{1 - 2\alpha x_1(1 - \nu_k^2) + i2\alpha x_2(1 - \nu_k^2)}{(1 - 2\alpha x_1(1 - \nu_k^2))^2 + 4\alpha^2 x_2^2(1 - \nu_k^2)^2}. \quad (25)$$

Obviously, the spectral function and hence the DOS are finite when  $x_2 \neq 0$ .

A simple analysis of Eq.(24) shows that the solution with  $x_2 = 0$  exists only for  $|\omega| > \omega_{max} = 2.97\tilde{t}\sqrt{2S}$  (or  $\alpha < \alpha_{cr} = 0.448$ ). At the critical point, we obtain  $x_1 = 0.43$ . For smaller frequencies Eq.(24) yields a solution with finite imaginary part, just as we found with the toy model with momentum independent  $\Psi$ . The total bandwidth is equal to  $W = 2\omega_{max} \approx 6\tilde{t}\sqrt{2S}$  upto corrections of order  $O(JS)$  which we neglected. For  $\omega$  only slightly below  $\omega_{max}$ , we have

$$x_2 \sim \sqrt{\omega_{max} - \omega}. \quad (26)$$

Substituting this into Eq.(25), we obtain that the DOS behaves near  $\omega_{max}$  as

$$N(\omega) \sim \frac{1}{\tilde{t}\sqrt{S}} \left( \frac{\omega_{max} - \omega}{\omega_{max}} \right)^{1/2}. \quad (27)$$

The above results are valid only as long as one can neglect the magnon dispersion. We now estimate the range of validity of this approximation. Recall that in transforming Eq.(13) into Eq.(14), we omitted the term

$$\int \frac{d^2q}{4\pi^2} \Psi(k, q - k)[G(q, \omega + \omega_q) - G(q, \omega)]. \quad (28)$$

Far from  $\omega_{max}$ , we do not expect this term to be relevant. Near the maximum frequency,  $G(\omega) - G(\omega_{max}) \propto (\omega_{max} - \omega)^{1/2}$ , and  $\partial G/\partial \omega$  is singular. Substituting the form of  $G$  from Eq.(25) with  $x_2$  from Eq.(26) into Eq.(28) we find that the term we omitted can be neglected when  $|\omega_{max} - \omega| \geq J^2 S^{5/2} \tilde{t}/(\omega_{max} - \omega)^2$ , i.e., when  $|\omega_{max} - \omega| \geq \Lambda$  where  $\Lambda = JS(\tilde{t}/J\sqrt{S})^{1/3}$ . At frequencies closer to  $\omega_{max}$ , the magnon dispersion is not negligible, and the calculation of the spectral function should be done using the full self-consistency equation Eq.(13). We will proceed with this calculation in the next section.

## B. Coherent part of the excitation spectrum

In this section, we study the form of the quasiparticle Green's function close to the top of the valence band, i.e., in the region  $|\omega_{max} - \omega| \leq \Lambda$ .

It is again instructive to consider first a toy model with a momentum independent interaction. Assume that typical value of the magnon frequency is  $\tilde{J}S$  with  $\tilde{J}/J = O(1)$ . We then have instead of Eq.(15)

$$G^{-1}(\omega) = \omega - \tilde{t}^2 SG(\omega + \tilde{J}S). \quad (29)$$

In the vicinity of  $\omega_{max}$ , the solution of this equation is

$$G(\omega) \approx \frac{2}{\omega_{max}} \left( 1 + \left( \frac{2}{\omega_{max}} \right)^{1/2} \frac{((\omega - \omega_{max})^3 + \tilde{\Lambda}^3)^{1/2}}{|\omega - \omega_{max}|} \right) \quad (30)$$

where  $\omega_{max} = 2\tilde{t}\sqrt{S} + O(\tilde{J}S)$  and  $\tilde{\Lambda} = \tilde{J}S(\tilde{t}/\tilde{J}\sqrt{S})^{1/3}$ . We see that there are two typical scales introduced by  $\tilde{J}$ . For  $|\omega - \omega_{max}| \geq \Lambda$ ,  $G(\omega)$  in Eq.(30) differs from that in Eq.(16) only by small corrections. For  $JS \leq |\omega - \omega_{max}| \leq \Lambda$ , the frequency dependence of the full solution is different from that in Eq.(16), however,  $G(\omega)$  remains approximately equal to  $2/\omega_{max}$ . Finally, at  $|\omega - \omega_{max}| \leq \tilde{J}S$ , the full Green's function begin to increase, and very near  $\omega_{max}$  we have

$$G(\omega) \approx \frac{\tilde{J}\sqrt{S}}{\tilde{t}} \frac{1}{\omega - \omega_{max}}. \quad (31)$$

We see that very near  $\omega_{max}$ , the Green's function has a conventional pole with the residue  $Z = \tilde{J}\sqrt{S}/\tilde{t}$ . This implies that around  $\omega_{max}$ , there should exist coherent fermionic excitations.

We now proceed with the solution of the actual self-consistency equation with a momentum-dependent  $\Psi(k, q - k)$ . Inspired by the solution of the toy model, we assume that there exists a frequency,  $\omega_{max}$  for which  $G^{-1}(k, \omega_{max}) = 0$  at some  $k = k_0$ , and which differs from the previously found onset frequency only by an amount of  $O(JS)$ . We will not be able to fully verify this assumption analytically as it would require us to find a solution

of Eq.(13) for all  $k$  and  $\omega \sim \omega_{max}$  which we cannot do. However, we will later verify this assumption in our numerical studies. We also assume and then verify that  $k_0 = (\pi/2, \pi/2)$ , and that near  $k = k_0$  and  $\omega = \omega_{max}$ , the excitations are mostly coherent, and the quasiparticle Green's function has the form

$$G(k, \omega) = \frac{Z}{\omega - \omega_{max} + E_k - i\gamma(\omega - \omega_{max})^2 \Theta(\omega - \omega_{max})}. \quad (32)$$

Here  $Z_k$  is the quasiparticle residue,  $\gamma$  is the damping coefficient,  $\Theta(x) = 1(0)$  if  $x < 0$  ( $x > 0$ ), and the hole excitation spectrum has the form

$$E_k = \frac{(k_\perp - k_0)^2}{2m_\perp} + \frac{(k_\parallel - k_0)^2}{2m_\parallel}, \quad (33)$$

where  $k_\perp, k_\parallel$  are the momenta along the boundary of the MBZ and along the zone diagonal, respectively.

In addition, as we discussed above, we introduce an upper cutoff  $q_c \leq 1$  in the integration over the magnon momentum, and restrict with an expansion of the magnon energy upto linear order in  $q$ . We recall that physically, the presence of this cutoff reflects the experimental fact that the zone-boundary magnons cease to exist as well-defined quasiparticles and therefore effectively do not contribute to the self-energy of the valence fermions. We will see that the quasiparticle residue  $Z$  scales as  $(q_c)^{-1/2}$ , but the effective masses are independent of  $q_c$ .

We now substitute the coherent ansatz for  $G(k, \omega)$  into the self-consistency equation Eq.(13). Expanding around  $k_0$  and  $\omega_{max}$  and using the fact that  $G^{-1}(k_0, \omega_{max}) = 0$ , we obtain self-consistent solutions for the quasiparticle residue, the quasiparticle spectrum and the damping coefficient. Consider first the quasiparticle residue. Setting  $k = k_0$  and expanding the r.h.s. of the self-consistency equation Eq.(13) to linear order in  $\omega_{max} - \omega$  we obtain

$$\frac{1 - Z}{Z} = \int \frac{d^2 q}{4\pi^2} \Psi(k_0, q) \frac{Z}{(\omega_q + E_{k_0+q})^2}, \quad (34)$$

where the integration runs upto  $q_c$ . Since  $q_c \ll 1$ , we can expand the two terms in the denominator to linear order in  $q$ . As  $\omega_q \propto q$  and  $E_{k_0+q} \propto q^2$ , the first term is dominant. Performing the integration with only  $\omega_q$  in the denominator, we obtain

$$1 = Z + \frac{\sqrt{2}\bar{t}^2 Z^2 q_c}{\pi J^2 S}. \quad (35)$$

In the limit  $J\sqrt{S}/t \ll 1$ , the term linear in  $Z$  can be neglected and we find

$$Z = \frac{J\sqrt{S}}{\bar{t}} \left( \frac{\pi\sqrt{2}}{q_c} \right)^{1/2}. \quad (36)$$

We see that  $Z$  scales linearly with  $J\sqrt{S}/t$  as in our toy model. This dependence was also obtained in earlier

studies [2]. It was however noticed in Ref. [3] that the linear dependence exists only for very small  $J/t$ . These authors argued that for moderate  $J/t$ ,  $Z \sim (J/t)^{1/2}$ . We also found deviations from the linear behavior already for moderately small  $J/t$ , however, we did not find a square root dependence for intermediate  $J/t$ . A plot of  $Z$  versus  $J/t$  is presented in Figs. 6 and 7.

Next, we calculate the quasiparticle damping coefficient  $\gamma$ . For this we again set  $k = k_0$ , neglect  $E_{k_0+q}$  compared to  $\omega_q$ , but do not expand in  $\omega - \omega_{max}$ . However, since we are interested in small deviations from  $\omega_{max}$  we can neglect the damping term on the r.h.s. of Eq.(13) compared to  $\omega - \omega_{max}$ . The r.h.s. of the self-consistency equation then takes the form

$$\int \frac{d^2 q}{4\pi^2} \Psi(k_0, q) \frac{Z}{\omega - \omega_{max} + \omega_q + i\delta}. \quad (37)$$

Clearly, for  $\omega > \omega_{max}$ , the denominator is positive and the integral does not contain an imaginary part. For  $\omega < \omega_{max}$ , however, the integrand has a pole at  $\omega = \omega_{max} - \omega_q$ . Integrating around the pole, we obtain a finite imaginary part which in 2D scales as  $(\omega - \omega_{max})^2$ . After performing the explicit calculations, we obtain

$$\gamma = \frac{\bar{t}^2 Z^2}{(2S)^2 J^3}. \quad (38)$$

The same result was obtained earlier by Kane, Lee and Read [2]. Note in passing that in contrast to a recent claim in Ref. [17], we did not find a missing factor of 2 in their formula. Substituting the expression for  $Z$  into Eq.(38), we finally obtain

$$\gamma = \frac{1}{4JS} \frac{\pi\sqrt{2}}{q_c}. \quad (39)$$

Comparing now the damping term with the term linear in frequency, we find that the fermionic excitations are weakly damped for  $E_k = \omega_{max} - \omega \leq 4JS(q_c/\pi\sqrt{2})$ . For small  $q_c$ , this condition is satisfied only in a small region around  $k_0$ . For example, for  $q_c = \sqrt{\pi/2}$  and  $m^{-1} \sim 4JS$ , the fermionic excitations are only weakly damped for  $|k - k_0| < 0.75$  which constitutes only a small fraction of the MBZ. Away from this region, the damping term is dominant, and the spectral function should possess a broad maximum around  $\omega = E_k$  rather than a sharp quasiparticle peak. This is in full agreement with the data [30,31] which show that the spectral function measured in photoemission experiments possesses a clearly distinguishable quasiparticle peak only in the vicinity of  $k_0$ .

We now proceed with the calculation of the effective masses. For this we set  $\omega = \omega_{max}$  and expand in the magnon momentum. We restrict ourselves to the strong coupling limit  $J\sqrt{S} \ll \bar{t}$  and neglect the bare dispersion, which in this limit is completely overshadowed by the self-energy correction. We then obtain



$$\begin{aligned}
\frac{E_k}{Z} = & - \int \frac{d^2 q}{4\pi^2} \Psi(k_0, q) \\
& \times \left\{ G(\omega_{max} + \omega_q, k + q) - G(\omega_{max} + \omega_q, k_0 + q) \right\} \\
& - \int \frac{d^2 q}{4\pi^2} \left\{ \Psi(k, q) - \Psi(k_0, q) \right\} G(\omega_{max} + \omega_q, k_0 + q) \\
& - \int \frac{d^2 q}{2\pi^2} \left\{ \Psi(k, q) - \Psi(k_0, q) \right\} \\
& \times \left\{ G(\omega_{max} + \omega_q, k + q) - G(\omega_{max} + \omega_q, k_0 + q) \right\} \quad (40)
\end{aligned}$$

Expanding the quasiparticle Green's function, we obtain

$$\begin{aligned}
& G(\omega_{max} + \omega_q, k + q) - G(\omega_{max} + \omega_q, k_0 + q) = \\
& Z \frac{E_{k_0+q} - E_{k+q}}{(\omega_q + E_{k_0+q})^2} + Z \frac{(E_{k_0+q} - E_{k+q})^2}{(\omega_q + E_{k_0+q})^3} + \dots \quad (41)
\end{aligned}$$

where

$$E_{k+q} - E_{k_0+q} = \frac{k_\perp^2}{2m_\perp} + \frac{k_\parallel^2}{2m_\parallel} + \frac{k_\perp q_\perp}{m_\perp} + \frac{k_\parallel q_\parallel}{m_\parallel} \quad (42)$$

The expansion of  $\Psi(k, q)$  upto quadratic order in  $k$  and upto linear order in  $q$  yields

$$\begin{aligned}
\Psi(k, q) - \Psi(k_0, q) = & 32t^2 S \\
& \times \left\{ \frac{\sqrt{2}}{4} k_\perp^2 q \left( 1 - \frac{q_\perp^2}{q} \right) - k_\perp q_\perp - \frac{k_\parallel^2 q_\perp^2}{2\sqrt{2}q} \right\} \quad (43)
\end{aligned}$$

Inserting now these expressions into Eq.(40) and using the result for the quasiparticle residue, we find that one of the two contributions to the first term on the r.h.s. of Eq.(40) cancels out the  $E_k/Z$  term on the l.h.s. The remaining terms are all proportional to  $\Psi$ , and therefore the energy scale  $t$  drops completely out of the problem. The only remaining scale is given by  $\omega_q$ , and the inverse effective masses are therefore proportional to the spin-wave velocity. Furthermore, we found that the integrals over the magnon momentum in the remaining terms in Eq.(40) are confined to the upper limit of the  $q$ -integration, and all scale as  $q_c^2$ . Therefore, the cutoff  $q_c$  also drops out of the problem. As a result, we obtain universal, model-independent equations for the masses

$$\begin{aligned}
\frac{3}{(4JSm_\perp)^2} - \frac{1}{JSm_\perp} + 1 &= 0, \\
\frac{1}{(4JSm_\parallel)^2} - 1 &= 0. \quad (44)
\end{aligned}$$

The second equation yields  $m_\parallel^{-1} = 4JS$ , while for  $m_\perp$  we obtain two solutions:  $m_\perp^{-1} = 4JS$  or  $\frac{4}{3}JS$ . We have checked that only the first solution for  $m_\perp$  can be continuously connected with the perturbative solution at weak

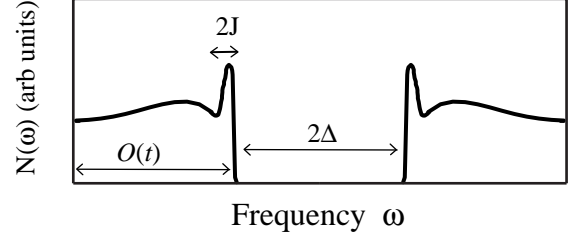


FIG. 4. The schematic form of the DOS at half-filling. The DOS reaches a maximum at energies  $\sim JS$ , below the gap, then drops down at slightly larger energies, and then gradually increases and saturates at energies which are  $\sim t$  away from the gap.

coupling. Then only the first solution is physically relevant, and we finally obtain

$$m_\parallel = m_\perp = (4JS)^{-1} \quad (45)$$

We see that in the limit  $q_c \ll 1$  and for  $J\sqrt{S}/t \ll 1$  when the bare dispersion can be neglected, the effective masses are equal, i.e., the top of the valence band is isotropic. This result is an intrinsic property of the Hubbard (or  $t - J$ ) model at strong coupling, independent of the form of the bare hopping. Note that the value of the masses is exactly the same as in the mean-field theory with  $t' = -0.5J$ .

We also estimated the magnitude of the corrections to this universal result for the masses. We indeed found that as  $q_c$  increases, the dispersion becomes anisotropic with  $m_\perp > m_\parallel$ . This trend is consistent with the results of other authors who integrated over the full magnetic Brillouin zone in Eq.(13) [3,8,11]. Finally, the form of the coherent part of the Green's function in Eq.(32) implies that the DOS behaves as  $(\omega_{max} - \omega)^2$  very near  $\omega_{max}$  and reaches the value

$$N \sim \frac{Z}{JS} \sim \frac{1}{t\sqrt{S}} \quad (46)$$

at  $\omega_{max} - \omega \sim JS$ , which is the largest scale where this form is applicable. At even larger frequencies, the DOS scales as

$$N \sim \frac{Z}{\omega_{max} - \omega} \quad (47)$$

and transforms into the fully incoherent DOS given by Eq.(27) at  $\omega_{max} - \omega \sim \Lambda$ . This incoherent density of states then gradually increases with frequency and saturates at  $\omega \ll \omega_{max}$ . These results imply that the DOS reaches a maximum at  $\omega_{max} - \omega \sim JS$ , then drops down at slightly larger frequencies  $\sim \Lambda$ , and then gradually increases and passes through a broad maximum at  $\omega \ll \omega_{max}$ . The behavior of the DOS is presented in Fig. 4. This behavior is in agreement with the numerical results which also find a strong coherent peak in the DOS at  $\omega_{max} - \omega \sim J$  on top of a smooth incoherent background [47].

### C. Vertex corrections

Finally, we consider the effect of vertex corrections. We already found in Sec. II that these corrections do not introduce any new scale, but at the same time they do not possess a factor of  $1/S$  and therefore can only be neglected due to a numerical smallness. To estimate the magnitude of the vertex renormalization, we computed the lowest-order vertex correction shown in Fig. 2 with the full quasiparticle Green's functions from Eq.(32). We followed the same computational steps as before, i.e., expanded to linear order in the magnon momentum and integrated upto  $q_c$ . Performing these calculations, we obtain that at small external momenta the full vertex has the same functional form as the bare one and differs from it by a factor  $(1 + \delta)$  where

$$\delta = \left( \frac{\sqrt{2}t^2 Z^2 q_c}{2\pi J^2 S} \right)^2 I \quad (48)$$

and

$$I = \int_0^1 dx \int_0^1 dy \frac{xy}{(x+y)^2} = (\log 2 - 0.5) \approx 0.2. \quad (49)$$

Substituting Eq.(36) for  $Z$  into Eq.(48), we obtain that the term in brackets is equal to unity, i.e.,  $\delta = I \approx 0.2$ . We see that the leading vertex correction accounts for only a 20% renormalization of the bare vertex. We did not explicitly compute higher-order vertex corrections, but our estimates show that they are likely to be progressively smaller. We therefore estimate that our analytical and numerical results for the dispersion obtained without vertex corrections are valid with an accuracy of about 20%.

### IV. NUMERICAL RESULTS

We now proceed with the discussion of the full numerical solution of the self-consistency equation for the quasiparticle Green's function.

As in the previous section, we begin by considering in Sec. IV A the frequency range  $|\omega - \omega_{max}| \gg \Lambda$ , in which the spectrum is completely incoherent. In Sec. IV B we then consider frequencies close to  $\omega_{max}$  for which we obtain coherent excitations on the scale of  $O(JS)$ . We present the results for the dispersion of a single hole for different values of  $J/t$  and  $t'/t$ , as well as different cutoffs  $q_c$ . For comparison with earlier studies we also present the results for the case when the magnons are considered as free particles.

We will demonstrate that for  $t' = 0$ , one recovers two equal effective masses only for very large  $t/J$ . However, after including a nearest-neighbor hopping  $t' = -0.5J$ , we obtain two roughly equal masses for all values of  $t/J$ . In this situation, the only effect of the decrease of  $J/t$

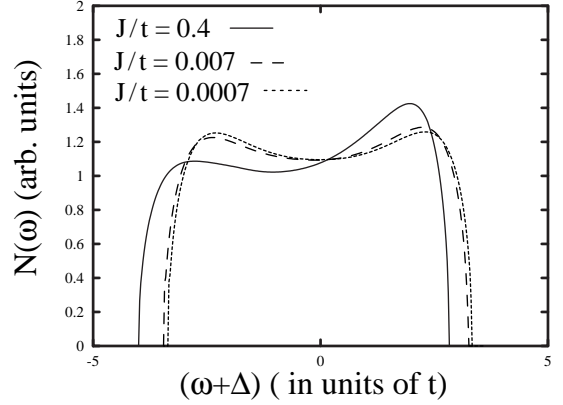


FIG. 5. The incoherent part of the hole excitation spectrum for several values of  $J/t$  (solid line  $J/t = 0.4$ , dashed line  $J/t = 0.007$  and dotted lines  $J/t = 0.0007$ ).

is the transfer of the spectral weight from the coherent to the incoherent part of the dispersion. Furthermore, for the experimentally relevant case  $J/t = 0.4$ , we find  $m^{-1} \approx (4JS)^{-1}$ . For  $S = 1/2$  this yields  $m^{-1} \approx (2J)^{-1}$ , which is the same value that was obtained in the photoemission experiments on  $Sr_2CuO_2Cl_2$ .

#### A. Incoherent part of the excitation spectrum

As we discussed in Sec. III A, for  $|\omega - \omega_{max}| \gg \Lambda$  we can neglect the magnon dispersion on the r.h.s of Eq.(11) and consider an integral equation only in momentum space. Following the same argument we also neglected the bare fermionic dispersion in Sec. III A. For our numerical studies, however, we kept the bare fermionic dispersion in order to illustrate how the DOS evolves with  $J/t$ . In Fig. 5 we present for several values of  $J/t$  the DOS resulting from the numerical solution of Eq.(14) for  $S = 1/2$  and  $t' = 0$ . We see that for intermediate  $J/t = 0.4$  (solid line), the DOS is asymmetric around  $\omega = 0$  with the density shifted towards negative frequencies. This indicates that the contribution from the bare dispersion which by itself yields a finite DOS only for negative  $\omega$  is not negligible. With decreasing  $J/t$  the asymmetry becomes weaker, until it basically vanishes for  $J/t = 0.007$ . This result is expected since in the limit  $J/t \rightarrow 0$  the bare dispersion becomes irrelevant, and we should recover a symmetric DOS. We also found that the total bandwidth only weakly depends on  $J/t$  and is roughly equal to  $W = 6.6t$ . This value is only slightly larger than  $W = 6t$  which we obtained analytically in Sec. III A.

#### B. Coherent part of the excitation spectrum

In order to solve Eq.(11) for the full Green's function we use a discrete mesh in frequency and in  $k$ -space.

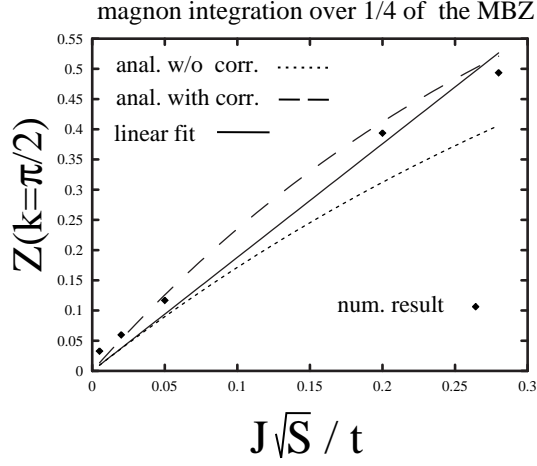


FIG. 6.  $Z$  as a function of  $J/t$ . The dotted and solid lines are the plots of Eqs.(35) and (36), respectively. The dashed line is our analytical result with subleading corrections in  $q_c$ . The filled diamonds are our numerical results. The integration over magnon momenta is restricted to 1/4 of the MBZ.

We assume that near the top of the valence band the quasiparticle Green's function has the form presented in Eq.(32) and obtain the onset frequency  $\omega_{max}$  and the hole dispersion  $E_k$  from the conditions

$$\begin{aligned} G^{-1}(k = k_0, \omega = \omega_{max}) &= 0, \\ G^{-1}(k, \omega = \omega_{max}) &= E_k/Z. \end{aligned} \quad (50)$$

To obtain the quasiparticle residue, we compute  $G^{-1}(k = k_0, \omega)$  and use the relation

$$Z = \frac{\Delta\omega}{G^{-1}(k, \omega_{max} + \Delta\omega) - G^{-1}(k, \omega_{max})}, \quad (51)$$

where  $\Delta\omega$  is a small shift from the maximal frequency. The dispersion extracted from Eq.(50) is formally valid only in the vicinity of  $k_0$ . At larger distances from  $k_0$ ,  $E_k$  does not necessary coincide with the position of the maximum in the spectral function due to a strong quasiparticle damping. In our numerical procedure for solving the self-consistency equation, we relate the Green's function at a given frequency  $\omega$  to the Green's functions at larger  $\omega + \omega_q$ , and progressively compute  $G$  at smaller and smaller  $\omega$ . Using this method, we cannot obtain the imaginary part of the full Green's function and therefore are unable to compare  $E_k$  extracted from Eq.(50) with the position of the maximum in the spectral function. We just assume without proof that at least not too far from  $k_0$ ,  $E_k$  and the peak position roughly coincide.

We first present in Figs. 6 and 7 our results for the quasiparticle residue at  $k = k_0 = (\pi/2, \pi/2)$  as a function of  $J/t$ . We have chosen two values of  $q_c$ : a smaller one  $q_c = \sqrt{2}\pi/16$  and a larger one for which the integration over the magnon momenta runs over 1/4 of the MBZ.

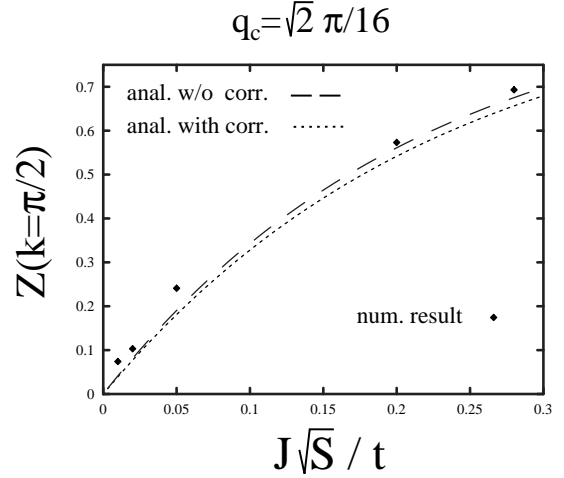


FIG. 7. The same as in Fig. 6 for  $q_c = 2^{1/2}\pi/16$ .

The squares in these figures represent our numerical results, the dotted line is our analytical formula, Eq.(36), obtained to leading order in  $q_c$ , and the dashed line incorporates subleading corrections in  $q_c$ . We see that for smaller  $q_c$ , the agreement between the numerical data and the results to leading order in  $q_c$  is rather good. For larger  $q_c$ , subleading corrections are more relevant. In both cases, however, the quasiparticle residue is substantially reduced from its value  $Z = 1$  for free fermions already for moderate  $J/t$ . We also see that the linear dependence exists only for very small  $J/t$  (see linear fit in Fig. 6).

In Fig. 8 we present the results for the ratio of the masses as a function of  $t/J$  for  $t' = 0$  and  $t' = -0.5J$ , respectively. In both cases, the integration over the magnon momenta runs over 1/4 of the MBZ. We see that for both values of  $t'$ , the ratio of the masses approaches one in the limit  $t/J \rightarrow \infty$ . This is in full agreement with our analytical results. We also see, however, that for  $t' = 0$ , one needs very large, unphysical values of  $t/J$  to recover the limiting behavior. For  $t' = -0.5J$ , the ratio of the masses is equal to one already at the mean-field level, and our results demonstrate that the ratio remains roughly equal to one for all values of  $t/J$  including the experimentally relevant  $t/J = 2.5$ . In order to see the effect of the  $J/t$  ratio on the whole fermionic dispersion, we present the results for  $E(k)$  for  $t' = 0$  and two different values of  $J/t$  in Fig. 9. We clearly see that the variation of  $J/t$  mainly affects the dispersion around  $(0, \pi)$ . The excitation energy in this region increases with  $t/J$ , i.e., the dip in the dispersion becomes deeper, which immediately leads to a decrease in the ratio of the effective masses. At the same time, the overall bandwidth only slightly increases with decreasing  $J/t$ . In Fig. 10 we compare the results for the fermionic dispersion for  $J/t = 0.4$  and for two values of  $t'$ ,  $t' = 0$  and  $t' = -0.4J$  (here the magnon integration runs over 1/4 of the MBZ). We see that for

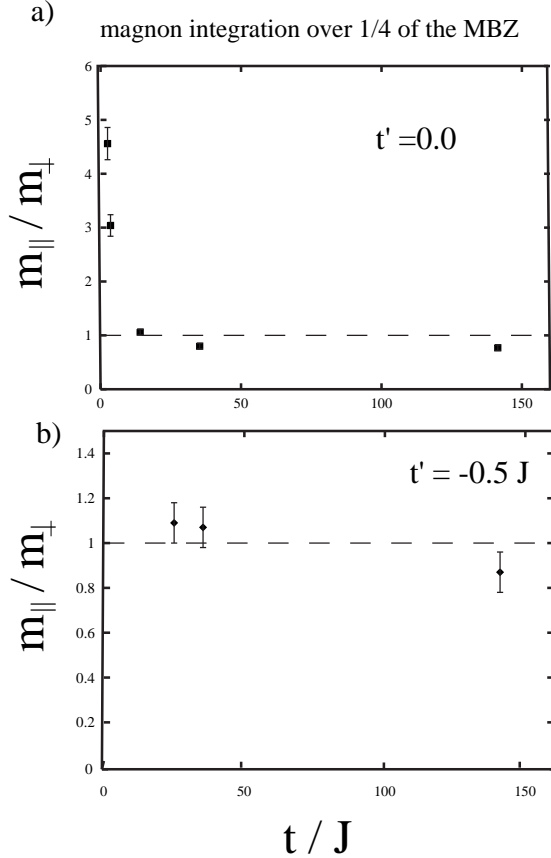


FIG. 8. The ratio of the effective masses  $m_{\perp}$  and  $m_{\parallel}$  as a function of  $t/J$  for (a)  $t' = 0$  and (b)  $t' = -0.5J$ . The integration over the magnon momenta runs over 1/4 of the MBZ.

$t' = 0$ , the dispersion is rather anisotropic and inconsistent with the experimental data [30,31]. On the contrary, for  $t' = -0.4J$ , not only the masses are equal, but also the energies at  $(0,0)$  and  $(0,\pi)$  are nearly equal to each other, and the bandwidth for coherent excitations is about  $3J$ . All three of these results are in full agreement with the data [30,31]. We also found that the energy at  $(0,\pi/2)$  is about half of that at  $(0,0)$  which agrees with the most recent data by LaRosa *et al* [31]. The results for  $t' = -0.5J$  are similar to those for  $t' = -0.4J$  and are presented in Fig. 11. In this figure we compare the dispersion for  $t' = -0.5J$  for two different ranges of integration over the magnon momentum. We see that while the integration over 1/4 of the MBZ yields a dispersion roughly consistent with the data, the integration over the full MBZ yields a highly anisotropic dispersion. However, one can increase  $t'$  even further and reduce the energy at  $(0,\pi)$  thus making the dispersion near  $(\pi/2,\pi/2)$  more isotropic even for the integration over the full MBZ. We illustrate this in Fig. 12 where we present the results for the fermionic dispersion for  $t' = -J$  and for the integra-

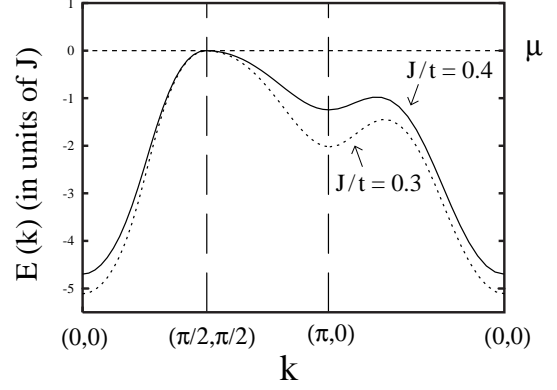


FIG. 9. The fermionic dispersions for  $t' = 0.0$  and two different values for  $J/t$  (solid line  $J/t = 0.4$ , dotted line  $J/t = 0.3$ ). The magnon integration is restricted to 1/4 of the MBZ.

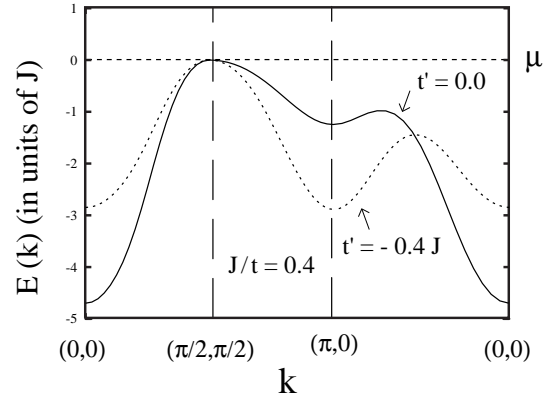


FIG. 10. The fermionic dispersions for  $J/t = 0.4$  and two different values for  $t'$  (solid line  $t' = 0.0$ , dotted line  $t' = -0.4J$ ). The magnon integration is restricted to 1/4 of the MBZ.

tion over the full MBZ. We see, however, that the overall bandwidth is still larger than in the experiments. We therefore conclude that if the integration over magnon momentum runs over the full MBZ (which implies that magnons are treated as free particles), the dispersion is inconsistent with the data for all reasonable values of  $t'$ . In this situation, to account for the data one has to adjust the hopping to even further neighbors.

For completeness, we also present several results for the integration over the full MBZ in the conventional  $t - J$  model without the three-cite term. This corresponds to neglecting the bare fermionic dispersion in Eq.(11). In Fig. 13 we present the results for the excitation energy for  $t' = 0$  and  $J/t = 0.4$ . This form of the dispersion is in very good agreement with the results of earlier studies [3,8,11]. As in previous studies, we found that the effective mass along the zone diagonal is roughly 7 times smaller than the mass along the boundary of the MBZ.

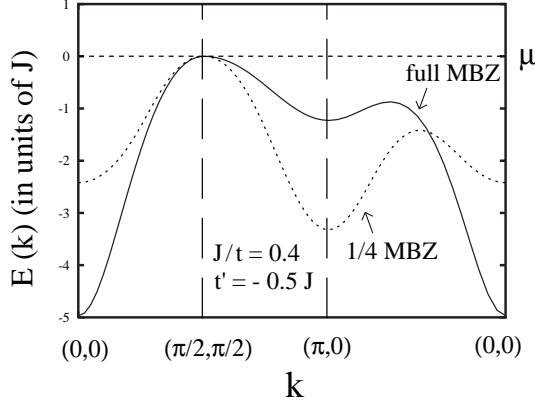


FIG. 11. The fermionic dispersions for  $J/t = 0.4$  and  $t' = -0.5J$  and two different ranges of integration. The solid and dotted lines are the results for the integration over the full MBZ and 1/4 of the MBZ, respectively.

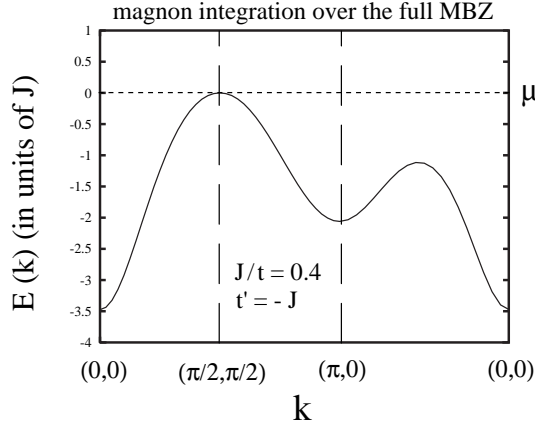


FIG. 12. The fermionic dispersions for  $J/t = 0.4$  and  $t' = -J$ . The integration over magnon momenta extends over the full MBZ.

In Fig. 14 we present the results for the evolution of the dispersion with  $t'$ . We see that as  $t'$  increases, the effective mass along  $(0, \pi)$  direction gets smaller. However, a rather large  $|t'|$  is needed to reproduce two equal masses. Moreover, for equal masses, the overall bandwidth is about two times smaller than in the experiments. We see again that without restricting the integration over magnon momentum, one needs to add and to fine tune the hopping parameters to even further neighbors to reproduce the experimental data.

## V. SUMMARY

We now summarize the results of our studies. We considered in this paper the dispersion of a single hole injected into a quantum antiferromagnet. We applied a spin-density-wave formalism extended to large number of

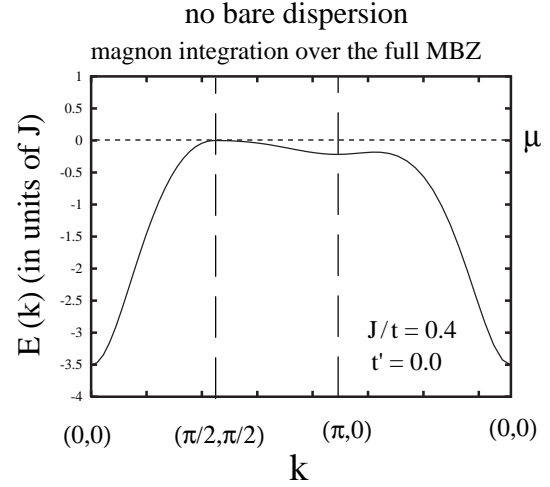


FIG. 13. The fermionic dispersion in the  $t - J$  model for  $J/t = 0.4$  and  $t' = 0$ . The integration over magnon momenta runs over the full MBZ.

orbitals  $n = 2S$ , and obtained an integral equation for the full quasiparticle Green's function in the self-consistent “non-crossing” Born approximation. At  $S = \infty$ , the mean-field theory is exact. At finite  $S$ , we found that the self-energy correction to the mean-field formula for  $G(k, \omega)$  scales as  $\bar{t}/J\sqrt{S}$ , and for large  $\bar{t}/J$ , relevant to experiments, is small only in the unphysical limit of a very large spin. We found that for  $\bar{t}/J\sqrt{S} \gg 1$ , the bare fermionic dispersion is completely overshadowed by the self-energy corrections. In this case, the quasiparticle Green's function contains a broad incoherent continuum which extends over a frequency range of  $\sim 6t$ . In addition, there exists a narrow region of width  $O(JS)$  below the top of the valence band, where the excitations are mostly coherent, though with a small quasiparticle residue  $Z \sim J\sqrt{S}/\bar{t}$ . The top of the valence band is located at  $(\pi/2, \pi/2)$ .

We found that the form of the fermionic dispersion, and, in particular, the ratio of the effective masses near  $(\pi/2, \pi/2)$  strongly depend on the assumptions one makes for the form of the magnon propagator. For free magnons, the integration over magnon momenta in the self-energy runs over the whole MBZ. In this case, we found, in agreement with earlier studies, that the dispersion around  $(\pi/2, \pi/2)$  is anisotropic with a much smaller mass along the zone diagonal. This result holds even if the bare dispersion contains a sizable  $t'$  term.

We, however, argued in the paper that the two-magnon Raman scattering [23] as well as neutron scattering experiments [36] strongly suggest that the zone boundary magnons are not free particles since a substantial portion of their spectral weight is transformed into an incoherent background. Most probably, this transformation is due to a strong magnon-phonon interaction. In this situation, only magnons with small momenta, for which the interac-



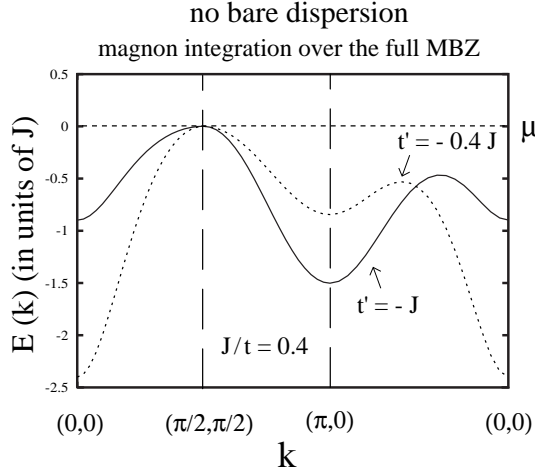


FIG. 14. The fermionic dispersion within the  $t - J$  model for  $J/t = 0.4$  and for two different values of  $t'$  (dotted line  $t' = 0.4J$ , solid line  $t' = -J$ ). The integration over magnon momenta runs over the full MBZ.

tion with phonons is necessary small, actually contribute to the self-energy. We modeled this effect by introducing a cutoff  $q_c$  in the integration over magnon momenta. We found analytically that for small  $q_c$ , the strong coupling solution for the Green's function is universal, and both of the effective masses are equal to  $(4JS)^{-1}$ . We further studied numerically the shape of the dispersion for intermediate  $J/t$  and found that for  $t' \sim -0.5J$  the ratio of the masses remains roughly equal to one for basically all values of  $J/t$ . This particular value for  $t'$  is obtained from a comparison of the low energy excitations in the underlying three-band model and the effective one-band Hubbard model [34]. We computed the full fermionic dispersion for  $J/t = 0.4$  relevant for  $Sr_2CuO_2Cl_2$ , and  $t' = -0.4J$  and found that not only the masses are both equal to  $(2J)^{-1}$ , but also the energies at  $(0, 0)$  and  $(0, \pi)$  are equal, the energy at  $(0, \pi/2)$  is about half of that at  $(0, 0)$ , and the bandwidth for the coherent excitations is around  $3J$ . All of these results are in full agreement with the experimental data by LaRosa *et al* [31] and also by Wells *et al* [30] (except for a slightly smaller bandwidth and larger energy at  $(0, \pi)$ ). Finally, we computed the damping of the coherent fermionic excitations and found that it is small only in a narrow range around  $(\pi/2, \pi/2)$ . Away from the vicinity of  $(\pi/2, \pi/2)$ , the excitations are overdamped, and the spectral function possesses a broad maximum rather than a sharp quasiparticle peak. This last feature was also reported in the photoemission experiments.

One of the goals of the present paper was to demonstrate that the experimental data for  $Sr_2CuO_2Cl_2$  can be described without introducing a spin-charge separation. In this respect, we predict that the data should not change much if the experiments are performed well below  $T_c$  though some anisotropy of the masses is possi-

ble because the spin damping decreases with decreasing  $T$  and hence  $q_c$  should become larger. This prediction is contrary to the one derived from a model with spin-charge separation [33]. In this last case, it was suggested that the minimal model with  $t' = 0$  already accounts for the key experimental features, and that well below  $T_c$ , spinons and holons are confined such that one should recover a strong anisotropy of the masses, similar to that in Fig. 13

A final remark. Though the point of departure of our analysis is very different from the one in the scenario based on spin-charge separation [33], in many respects there exists a striking similarity between the results obtained in both approaches. First, we found that the excitations are mostly incoherent, and the bandwidth of incoherent excitations is several  $t$ . Second, we obtained that the dispersing excitations observed in photoemission measurements exists upto an energy scale which is given by  $J$  rather than by  $t$ . Both of these results are in full agreement with the results obtained by Laughlin in the framework of spin-charge separation. However, contrary to Laughlin, we did find a conventional Fermi-liquid pole in  $G(k, \omega)$  near  $(\pi/2, \pi/2)$ . The quasiparticle residue of the coherent excitations is small in the strong coupling limit and vanishes when  $J/t \rightarrow 0$ . In view of these results, we suspect that spinons and holons are actually confined even above the Neel temperature, but the confinement is weak near  $(\pi/2, \pi/2)$  and disappears when  $J/t \rightarrow 0$ . A detailed study of this confinement is clearly called for.

It is our pleasure to thank G. Blumberg, E. Dagotto, R. Joynt, R. Laughlin, M. Onellion, Z-X. Shen and O. Sushkov for useful discussions. The work was supported by nsf-dmr 9629839 and by A.P. Sloan Fellowship (A. Ch).

- 
- [1] B. I. Shraiman and E. D. Siggia, Phys. Rev. Lett. **60**, 740 (1988); **61**, 467 (1988).
  - [2] C.L. Kane, P.A. Lee, and N. Read, Phys. Rev. B **39**, 6880 (1989).
  - [3] F. Marsiglio, A.E. Ruckenstein, S. Schmitt-Rink, and C.M. Varma, Phys. Rev. B **43**, 10882 (1991).
  - [4] J.R.Schrieffer, X.G.Wen, and S.C.Zhang, Phys. Rev. B **39**, 11663 (1989); A.V.Chubukov and D.M.Frenkel, Phys. Rev. B **46**, 11884 (1992).
  - [5] J. E. Hirsch, Phys. Rev. Lett. **54**, 1317 (1985) ; C. Gros, R. Joynt, and T. M. Rice, Phys. Rev. B **36**, 381 (1987).
  - [6] E. Dagotto, R. Joynt, A. Moreo, S. Bacci and E. Dagotto, Phys. Rev. B **41**, 9049 (1990).
  - [7] E. Dagotto, Rev. Mod. Phys. **66**, 763 (1994).
  - [8] E. Dagotto, A. Nazarenko and M. Boninsegni, Phys. Rev. Lett. **73**, 728 (1994); A. Nazarenko, K.J.E. Vos, S. Haas, E. Dagotto and R. Gooding, Phys. Rev. B **51**, 8676 (1995).

- [9] A. Singh and Z. Tešanović, Phys. Rev. B **41**, 11457 (1990).
- [10] G. Vignale and M.R. Hedayati, Phys. Rev. B **42**, 786 (1990).
- [11] M. Boninsegni and E. Manousakis, Phys. Rev. B **43**, 10353 (1991); Z. Liu and E. Manousakis, Phys. Rev. B **45**, 2425 (1992).
- [12] S. Trugman, Phys. Rev. B **37**, 1597 (1988).
- [13] S. Sachdev, Phys. Rev. B **39**, 12232 (1989).
- [14] V.I. Belinicher, A.L. Chernyshev and V.A. Shubin, Phys. Rev. B **54**, 14914 (1996).
- [15] A.V. Chubukov and K.A. Musaelian, Phys. Rev. B **50**, 6238 (1994).
- [16] D. Duffy and A. Moreo, Phys. Rev. B **52**, 15607 (1995).
- [17] B. Kyund and S.I. Mukhin, Phys. Rev. B **55**, 3886 (1997).
- [18] P.W. Leung and R.J. Gooding, Phys. Rev. B **52**, R15711 (1995); P.W. Leung, B.O. Wells and R.J. Gooding, unpublished
- [19] O.P. Sushkov, Phys. Rev. B **54**, 9988 (1996) and references therein.
- [20] see e.g., J. Bala, A.M. Oles and J. Zaanen, Phys. Rev. B **52**, 4597 (1995)
- [21] S.M. Hayden, G. Aeppli, H. Mook, D. Rytz, M.F. Hundley, and Z. Fisk, Phys. Rev. Lett. **67**, 3622 (1991).
- [22] T. Imai, C.P. Slichter, K. Yoshimura, and K. Kosuge, Phys. Rev. Lett. **70**, 1002 (1993).
- [23] G. Blumberg, P. Abbamonte, M.V. Klein, W.C. Lee, D.M. Ginsberg, L.L. Miller, and A. Zibold, Phys. Rev. B **53**, R11930 (1996) and references therein.
- [24] R.R.P. Singh, Comments Cond. Mat. Phys. **15**, 241 (1991).
- [25] K. Gofron et al, Phys. Rev. Lett. **73**, 3302 (1994); Jian Ma et al, Phys. Rev. B **51**, 3832 (1995); D.S. Marshall *et al.*, Phys. Rev. Lett. **76**, 4841 (1996)
- [26] Z-X Shen and J.R. Schrieffer, Phys. Rev. Lett., **78**, 1771 (1997).
- [27] A. Chubukov, D. Morr and K. Shakhnovich, Phil. Mag., **74**, 563 (1996).
- [28] A.V. Chubukov and D.K. Morr, Phys. Rep., to appear (1997).
- [29] J. Schmalian, D. Pines and B. Stojkovic, Phys. Rev. Lett, to appear.
- [30] B.O. Wells *et al.*, Phys. Rev. Lett. **74**, 964 (1995).
- [31] S. LaRosa *et al.*, Phys. Rev. B **56**, R525 (1997).
- [32] L.B. Ioffe and A.I. Larkin, Phys. Rev. B **39**, 8988 (1989); N. Nagaosa and P.A. Lee, Phys. Rev. Lett. **64**, 2450 (1990); P.A. Lee and X.-G. Wen, Phys. Rev. Lett. **76**, 503 (1996).
- [33] R.B. Laughlin, preprint cond-mat 9608005 and private communication.
- [34] M. S. Hybertsen, E. B. Stechel, M. Schluter, and D. R. Jennison, Phys. Rev. B **41**, 11068 (1990).
- [35] O.A. Starykh, O.F. de Alcantara Bonfim and G. Reiter, Phys. Rev. B **52**, 12534 (1995).
- [36] G. Aeppli, T.E. Mason, S.M. Hayden and H.A. Mook, preprint.
- [37] W.H. Weber and G.W. Ford, Phys. Rev. B **40**, 6890 (1989).
- [38] P. Knoll, C. Thomsen, M. Cardona, and P. Murugaraj, Phys. Rev. B **42**, 4842 (1990).
- [39] B.I. Halperin and P.C. Hohenberg, Phys. Rev. **188**, 898 (1969); D. Forster, *Hydrodynamic Fluctuations, Broken Symmetry, and Correlation Functions* (Benjamin/Cummings, Reading, MA, 1975)
- [40] P.W. Anderson and J.R. Schrieffer, Phys. Today **44**, 55 (1991).
- [41] D.J. Scalapino, Phys. Rep. **250**, 329 (1995) and references therein.
- [42] A.P. Kampf, Phys. Rep. **249**, 219 (1994).
- [43] I. Affleck and D. Haldane, Phys. Rev. B **36**, 5291 (1987).
- [44] A.V. Chubukov and D.M. Frenkel, Phys. Rev. Lett. **74**, 3057 (1995); Phys. Rev. B **52**, 9760 (1995).
- [45] S. Schmitt-Rink, C.M. Varma, and A.E. Ruckenstein, Phys. Rev. Lett. **60**, 2793 (1988).
- [46] see e.g., F. Lema and A.A. Aligia, Phys. Rev. B **55**, 14092 (1997).
- [47] R. Preuss, W. Hanke, and W. von der Linden, Phys. Rev. Lett. **75**, 1344 (1995).